Numer. Math. Theor. Meth. Appl.
doi: 10.4208/nmtma.OA-2021-0165

Vol. **15**, No. 2, pp. 279-303
May 2022

A Third Order Accurate in Time, BDF-Type Energy Stable Scheme for the Cahn-Hilliard Equation

Kelong Cheng[1], Cheng Wang[2,*], Steven M. Wise[3] and Yanmei Wu[1]

[1] *School of Science, Southwest University of Science and Technology, Mianyang, Sichuan 621010, P.R. China*
[2] *Department of Mathematics, The University of Massachusetts, North Dartmouth, MA 02747, USA*
[3] *Department of Mathematics, The University of Tennessee, Knoxville, TN 37996, USA*

Received 5 October 2021; Accepted (in revised version) 21 January 2022

Abstract. In this paper we propose and analyze a backward differentiation formula (BDF) type numerical scheme for the Cahn-Hilliard equation with third order temporal accuracy. The Fourier pseudo-spectral method is used to discretize space. The surface diffusion and the nonlinear chemical potential terms are treated implicitly, while the expansive term is approximated by a third order explicit extrapolation formula for the sake of solvability. In addition, a third order accurate Douglas-Dupont regularization term, in the form of $-A_0\Delta t^2\Delta_N(\phi^{n+1}-\phi^n)$, is added in the numerical scheme. In particular, the energy stability is carefully derived in a modified version, so that a uniform bound for the original energy functional is available, and a theoretical justification of the coefficient A becomes available. As a result of this energy stability analysis, a uniform-in-time L_N^6 bound of the numerical solution is obtained. And also, the optimal rate convergence analysis and error estimate are provided, in the $L^\infty_{\Delta t}(0,T;L^2_N)\cap L^2_{\Delta t}(0,T;H^2_h)$ norm, with the help of the L_N^6 bound for the numerical solution. A few numerical simulation results are presented to demonstrate the efficiency of the numerical scheme and the third order convergence.

AMS subject classifications: 35K30, 35K55, 65L06, 65M12, 65M70, 65T40

Key words: Cahn-Hilliard equation, third order backward differentiation formula, unique solvability, energy stability, discrete L_N^6 estimate, optimal rate convergence analysis.

1. Introduction

The Allen-Cahn (AC) [1] (non-conserved dynamics) and Cahn-Hilliard (CH) [4]

*Corresponding author. *Email addresses:* zhengkelong@swust.edu.cn (K. Cheng), cwang1@umassd.edu (C. Wang), swise1@utk.edu (S.M. Wise), wuyanmei@swust.edu.cn (Y. Wu)

(conserved dynamics) equations, are some of the best known gradient flow models. They result from the same or similar models for the free energy density and only differ in whether they are conserved or non-conserved flows. The CH equation model spinodal decomposition and phase separation in a binary alloy or fluid. Over a bounded domain $\Omega \subset \mathbb{R}^d$ (with $d = 2$ or $d = 3$), the Cahn-Hilliard energy functional is given by [4]

$$E(\phi) = \int_\Omega \left(\frac{1}{4}\phi^4 - \frac{1}{2}\phi^2 + \frac{1}{4} + \frac{\varepsilon^2}{2}|\nabla \phi|^2 \right) d\mathbf{x} \tag{1.1}$$

for any $\phi \in H^1(\Omega)$, where ε is a constant associated with the interface width. The CH equation is precisely the H^{-1} (conserved) gradient flow of the energy functional (1.1)

$$\phi_t = \Delta \mu, \quad \mu := \delta_\phi E = \phi^3 - \phi - \varepsilon^2 \Delta \phi. \tag{1.2}$$

Variations of the model may use non-constant mobilities or other free energy densities. For simplicity of presentation, we assume periodic boundary condition in this article, although an extension to other type boundary conditions, such as the homogeneous Neumann one, will be straightforward. Due to the gradient structure of (1.2), the following energy dissipation law holds:

$$\frac{d}{dt} E\big(u(t)\big) = -\int_\Omega |\nabla w|^2 d\mathbf{x}.$$

Furthermore, the equation is mass conservative, $\int_\Omega \partial_t u \, d\mathbf{x} = 0$, which follows from the conservative structure of the equation together with the periodic Neumann boundary conditions for μ. This property can be re-expressed as $(u(\,\cdot\,, t), 1) = (u_0, 1)$, for all $t \geq 0$.

The Cahn-Hilliard equation is a very important model in mathematical physics. It is often paired with equations that describe important physical behavior of a given physical system, typically through nonlinear coupling terms. Examples of such coupled models include the Cahn-Hilliard-Navier-Stokes (CHNS) equation for two-phase, immiscible flow; the Cahn-Larché model of binary solid state diffusion for elastic misfit; the Cahn-Hilliard-Hele-Shaw (CHHS) equation for spinodal decomposition of a binary fluid in a Hele-Shaw cell, etc. The scientific challenge of the CH equation model is obvious, due to its fourth-order, nonlinear parabolic-type nature.

The energy stability of a numerical scheme has been a very important issue, since it plays an essential role in the accuracy of long time numerical simulation. There have been extensive existing numerical works with energy stability, in particular for first order and second order accurate (in time) schemes. Among the second order energy stable numerical schemes, the temporal discretization has been focused on either the Crank-Nicolson approximation [7, 17–20, 26–30] or the second order backward differentiation formula (BDF) one [13, 47]. Other than these numerical algorithms for the Cahn-Hilliard model, which preserve the energy dissipation in the original phase variable, a few other numerical works have been reported for the reformulated physical system with an introduction of certain auxiliary variables, such as the scalar auxiliary

variable (SAV) approach [40–42]. In comparison with the first order schemes, the numerical viscosity is drastically reduced in these second order schemes, and this fact has been verified by both the theoretical analysis and various numerical experiments.

Furthermore, it is observed that, some artificial diffusion terms were contained in these reported second order accurate schemes to ensure the energy stability. In turn, a quantitative study of these numerical dissipations is needed to explore their impact on the long time numerical accuracy. Meanwhile, various numerical experiments have revealed that third order accurate schemes can drastically reduce the numerical dissipation and improve the long time numerical accuracy. For example, a recent work [14] of a third order scheme for the no-slope-selection (NSS) thin film gradient equation has produced much more accurate solutions than the ones computed by the second order schemes, in particular in terms of power law index for growth of the surface roughness and the mound width in the coarsening process, with improvements of two more decimal points in both power law index precisions. Also see [8, 31] for similar numerical results. Meanwhile, it is observed that, a theoretical analysis for these reported third order schemes for the no-slope-selection thin film model is based on the following subtle fact: the derivatives of the nonlinear terms in the NSS model are automatically L^∞, due to the special structure of the function $\ln(1+|\mathbf{x}|^2)$. On the other hand, such a nice property is not available for many gradient equations with a polynomial-pattern energy potential, such as the presently-considered Cahn-Hilliard flow. As a result, efficient and stable third order accurate numerical schemes are expected to be highly desirable in the scientific computing of Cahn-Hilliard type equations. But, another natural question arises: could the energy stability be theoretically justified for a third order accurate (in time) numerical scheme for Cahn-Hilliard model? In fact, this problem is open for the gradient flow with polynomial free energy. In the existing literature, the only related work in this category could be found in [46], where a linearized third order numerical scheme was used for the slope-selection epitaxial thin film equation. However, a theoretical justification of the energy stability analysis has not been available for the discussed numerical scheme, while the analyses for the first and second order accurate linearized schemes have been reported in [33–35].

In this article, we propose and analyze a third order accurate numerical scheme for the CH equation (1.2), based on the standard BDF3 temporal approximation, combined with an explicit extrapolation formula for the expansive linear term. The unique solvability analysis comes from the convexity structure associated with the nonlinear implicit term. Moreover, the explicit treatment to the linear expansive term would not be able to ensure the energy stability at the theoretical level. To overcome this difficulty, we have to add a third order Douglas-Dupont regularization term in the numerical scheme, namely in the form of $-A_0\Delta t^2\Delta_N(\phi^{n+1}-\phi^n)$. Furthermore, a careful energy estimate enables us to derive a rigorous stability estimate for a modified energy function, which contains the original energy functional and a few non-negative numerical correction terms. Meanwhile, the Fourier pseudo-spectral method is utilized for spatial approximation, and the discrete summation by parts property will facilitate the corresponding analysis for the fully discrete scheme. As a result of this modified en-

ergy stability, we are able to derive a uniform-in-time H_h^1 bound for the original energy functional, which in turn leads to an L_N^6 estimate for the numerical solution, with the help of a discrete Sobolev embedding.

In addition to the energy stability analysis, we provide a theoretical analysis with the optimal convergence rate, $\mathcal{O}(\Delta t^3 + h^m)$, for the proposed third order BDF3 scheme, in the $L_{\Delta t}^\infty(0,T;L_N^2) \cap L_{\Delta t}^2(0,T;H_h^2)$ norm. Similar to the estimates [31, 48], a direct inner product with the numerical error equation by e^{n+1} (the error function at time step t^{n+1}) does not lead to the desired result, because of the long stencil structure involved. Instead, an inner product with $e^{n+1} + (e^{n+1} - e^n)$ is considered by in the analysis, originated from an existing work [37]. In turn, the full order convergence result is expected via detailed numerical error estimates. In particular, the established uniform-in-time L_N^6 bound for the numerical solution will play an essential role in the convergence estimate.

The long time simulation results for the coarsening process have indicated a $t^{-\frac{1}{3}}$ law for the energy decay. In particular, the power index for energy decay, created by the proposed third order BDF scheme, is more accurate than those created by certain second order schemes in the existing literature, with the same numerical resolution. This experiment has demonstrated the robustness of the proposed BDF3 numerical scheme.

The rest of the article is organized as follows. In Section 2 we present the numerical scheme, including the review of the Fourier pseudo-spectral spatial approximation. Afterward, a modified energy stability is established for the proposed third order BDF scheme. Subsequently, the $L_N^\infty(0,T;L_N^2) \cap L_N^2(0,T;H_h^2)$ convergence estimate is provided in Section 3. In Section 4 we present the numerical results, including the accuracy test and the long time simulation for the coarsening process. Finally, the concluding remarks are given in Section 5.

2. The numerical scheme

2.1. Review of the Fourier pseudo-spectral approximation

For simplicity of presentation, we assume that the domain is given by $\Omega = (0, L)^2$, $N_x = N_y = N$ and $N \cdot h = L$. A more general domain could be treated in a similar manner. Furthermore, to facilitate the pseudo-spectral analysis in later sections, we set $N = 2K + 1$. (The case for N even can be treated similarly.) All the variables are evaluated at the regular numerical grid (x_i, y_j, z_k), with $x_i = ih$, $y_j = jh$, $z_k = kh$, $0 \le i, j, k \le 2K + 1$.

Without loss of generality, we assume that $L = 1$. For a periodic function f over the given 3D numerical grid, define its discrete Fourier expansion as

$$f_{i,j,k} = \sum_{\ell,m,n=-K}^{K} \hat{f}_{\ell,m,n} \exp\big(2\pi \mathrm{i}(\ell x_i + m y_j + n z_k)\big). \tag{2.1}$$

Then, the Fourier collocation spectral approximations to first and second order partial derivatives in the x-direction become

$$(\mathcal{D}_{Nx} f)_{i,j,k} = \sum_{\ell,m,n=-K}^{K} (2\ell\pi \mathrm{i})\, \hat{f}_{\ell,m,n} \exp\big(2\pi \mathrm{i}(\ell x_i + m y_j + n z_k)\big), \tag{2.2}$$

$$\big(\mathcal{D}_{Nx}^2 f\big)_{i,j,k} = \sum_{\ell,m,n=-K}^{K} \big(-4\pi^2 \ell^2\big)\, \hat{f}_{\ell,m,n} \exp\big(2\pi \mathrm{i}(\ell x_i + m y_j + n z_k)\big). \tag{2.3}$$

The differentiation operators in the y and z directions, namely, $\mathcal{D}_{Ny}$, $\mathcal{D}_{Ny}^2$, $\mathcal{D}_{Nz}$, $\mathcal{D}_{Nz}^2$, are defined in the same fashion. In turn, the discrete Laplacian, gradient and divergence become

$$\begin{aligned} &\Delta_N f = \big(\mathcal{D}_{Nx}^2 + \mathcal{D}_{Ny}^2 + \mathcal{D}_{Nz}^2\big)\, f, \\ &\nabla_N f = \begin{pmatrix} \mathcal{D}_{Nx} f \\ \mathcal{D}_{Ny} f \\ \mathcal{D}_{Nz} f \end{pmatrix}, \quad \nabla_N \cdot \begin{pmatrix} f_1 \\ f_2 \\ f_3 \end{pmatrix} = \mathcal{D}_{Nx} f_1 + \mathcal{D}_{Ny} f_2 + \mathcal{D}_{Nz} f_3, \end{aligned} \tag{2.4}$$

at the point-wise level. See the derivations in the related references [3, 5, 23, 32], etc.

We define the grid function space

$$\mathcal{G}_N := \big\{ f : \mathbb{Z}^3 \to \mathbb{R} \;\big|\; f \text{ is } \Omega_N\text{-periodic} \big\}. \tag{2.5}$$

The zero-mean grid function subspace is denoted

$$\mathring{\mathcal{G}}_N := \big\{ f \in \mathcal{G}_N \;\big|\; \langle f, 1\rangle =: \overline{f} = 0 \big\},$$

where

$$\langle f, g\rangle := h^3 \sum_{i,j,k=0}^{N-1} f_{i,j,k} g_{i,j,k} \tag{2.6}$$

for any $f, g \in \mathcal{G}_N$. The discrete form of the L^2 norm is defined as

$$\|f\|_2 := \sqrt{\langle f, f\rangle}. \tag{2.7}$$

A careful calculation yields the following formulas of summation by parts at the discrete level (see the related discussions [6, 10, 24, 25]):

$$\langle f, \Delta_N g\rangle = -\langle \nabla_N f, \nabla_N g\rangle, \quad \big\langle f, \Delta_N^2 g\big\rangle = \langle \Delta_N f, \Delta_N g\rangle. \tag{2.8}$$

For any grid function $f \in \mathring{\mathcal{G}}_N$, the operator $(-\Delta_N)^{-1}$ and the discrete $\|\cdot\|_{-1,N}$ norm are defined as

$$\big((-\Delta_N)^{-1} f\big)_{i,j,k} := \sum_{\ell,m,n \neq \mathbf{0}} \frac{1}{\lambda_{\ell,m,n}} \hat{f}_{\ell,m,n} \exp\big(2\pi \mathrm{i}(\ell x_i + m y_j + n z_k)\big), \tag{2.9}$$

$$\|f\|_{-1,N} := \sqrt{\langle f, (-\Delta_N)^{-1} f\rangle}, \tag{2.10}$$

where $\lambda_{\ell,m,n} := 4\pi^2(\ell^2 + m^2 + n^2)$.

In addition to the standard L_N^2 norm, we also introduce the L_N^p and discrete maximum norms for a grid function f, to facilitate the analysis in later sections

$$\|f\|_\infty := \max_{i,j,k} |f_{i,j,k}|, \quad \|f\|_p := \left(h^3 \sum_{i,j,k=0}^{N-1} |f_{i,j,k}|^p \right)^{\frac{1}{p}}, \quad 1 \le p < \infty. \tag{2.11}$$

The discrete H^1 norm is introduced as

$$\|f\|_{H_N^1}^2 := \|f\|_2^2 + \|\nabla_N f\|_2^2.$$

For any grid function ϕ, the discrete energy is defined as

$$E_N(\phi) = \frac{1}{4}\|\phi\|_4^4 - \frac{1}{2}\|\phi\|_2^2 + \frac{1}{4}|\Omega| + \frac{\varepsilon^2}{2}\|\nabla_N \phi\|_2^2 . \tag{2.12}$$

The following result corresponds to a discrete Sobolev embedding from H_N^1 to L_N^6 in the pseudo-spectral space. Similar discrete embedding estimates in the discrete L_N^4 and L_N^∞ norms could be found in [17, Lemmas 2.1 and 2.2]; a discrete embedding from H_N^2 to $W_N^{1,6}$ has been reported in [16]; also see the related results [9, 21, 22] in the finite difference version. A direct calculation is not able to derive this inequality; instead, a discrete Fourier analysis has to be applied in the derivation. The details will are given in Appendix A.

Proposition 2.1. *For any periodic grid function f, we have*

$$\|f\|_6 \le C\|f\|_{H_N^1} \tag{2.13}$$

for some constant $C > 0$ only dependent on Ω.

2.2. The proposed third order BDF numerical scheme

As usual, we denote ϕ^k as the numerical approximation to the PDE solution at time step $t^k := k\Delta t$, with any integer k. For $n \ge 2$, given ϕ^n, ϕ^{n-1}, ϕ^{n-2}, we propose a third order BDF-type scheme for the CH equation (1.2)

$$\begin{aligned} &\frac{1}{\Delta t}\frac{11}{6}\phi^{n+1} - 3\phi^n + \frac{3}{2}\phi^{n-1} - \frac{1}{3}\phi^{n-2} \\ &= \Delta_N\Big(\big(\phi^{n+1}\big)^3 - \big(3\phi^n - 3\phi^{n-1} + \phi^{n-2}\big) - \varepsilon^2 \Delta_N \phi^{n+1} - A_0 \Delta t^2 \Delta_N \big(\phi^{n+1} - \phi^n\big) \Big). \end{aligned} \tag{2.14}$$

Remark 2.1. Since the third order algorithm (2.14) is a three-step scheme, the numerical approximations ϕ^1 and ϕ^2 are needed in the initial time step. If we take $\phi^2 = \phi^1 = \phi^0$, the energy bound estimate will become simple, while the third order numerical accuracy may have been lost in the initial step. Instead, we could use alternate explicit high-order numerical algorithms, such as $RK2$ and $RK3$, to update

the numerical solutions at ϕ^1 and ϕ^2, so that the third order numerical accuracy is preserved in the first few time steps. This approach enables one to derive the full third order temporal convergence estimate, as will be demonstrated in the future sections. In particular, we notice that the first two RK time steps in the initial approximation will not cause any stability concern, since they are treated as the initial values in the numerical scheme.

For the proposed scheme (2.14), the mass-conservative property is always valid $\overline{u^{n+1}} = \overline{u^n} = \overline{u^0} := \beta_0$, which comes from the following obvious identity: $\overline{\Delta_N g} = 0$, for any periodic grid function g.

2.3. Unique solvability analysis

The unique solvability of the proposed numerical scheme (2.14) is stated in the following theorem.

Theorem 2.1. *For $n \geq 2$, given ϕ^n, ϕ^{n-1}, $\phi^{n-2} \in \mathcal{G}_N$, with $\overline{\phi^n} = \overline{\phi^{n-1}} = \overline{\phi^{n-2}} = \beta_0$, there is a unique solution $\phi^{n+1} \in \mathcal{G}_N$ to the proposed scheme* (2.14).

Proof. The numerical solution to (2.14) could be equivalently rewritten as

$$\mathcal{N}_N[\phi] = f := \Delta t\big(\hat{\phi}^{n+1} - A_0 \Delta t^2 \Delta_N \phi^n\big) \tag{2.15}$$

with

$$\hat{\phi}^{n+1} := 3\phi^n - 3\phi^{n-1} + \phi^{n-2},$$

and

$$\begin{aligned} \mathcal{N}_N[\phi] := (-\Delta_N)^{-1} \left(\frac{11}{6}\phi - 3\phi^n + \frac{3}{2}\phi^{n-1} - \frac{1}{3}\phi^{n-2} \right) \\ + \Delta t \phi^3 - \Delta t\big(\varepsilon^2 + A_0 \Delta t^2\big)\Delta_N \phi. \end{aligned} \tag{2.16}$$

By setting $\phi = \beta_0 + \tilde{\phi}$ (with $\beta_0 = \bar{\phi}$), the nonlinear equation (2.15) can be recast as a minimization problem for the following discrete energy functional:

$$\begin{aligned} F_N[\tilde{\phi}] := \frac{3}{11} \left\| \frac{11}{6}(\tilde{\phi} + \beta_0) - 3\phi^n + \frac{3}{2}\phi^{n-1} - \frac{1}{3}\phi^{n-2} \right\|_{-1,N}^2 + \frac{\Delta t}{4} \big\| \tilde{\phi} + \beta_0 \big\|_4^4 \\ + \frac{(\varepsilon^2 + A_0 \Delta t^2)\Delta t}{2} \big\| \nabla_N \tilde{\phi} \big\|_2^2 - \big\langle f, \tilde{\phi} + \beta_0 \big\rangle \end{aligned} \tag{2.17}$$

for any $\tilde{\phi} \in \mathring{\mathcal{G}}_N$. Since F_N it has a unique numerical minimizer. This is the unique solution for (2.14). □

2.4. The energy stability analysis

The energy stability of the proposed third order BDF-type scheme (2.14) is stated in the following theorem, in a modified version.

Theorem 2.2. *Suppose that $A_0 \geq \frac{9}{32}\varepsilon^{-2}$ and $n \geq 2$. The numerical solution produced by the proposed BDF-type scheme* (2.14) *satisfies*

$$\tilde{E}_N\big(\phi^{n+1}, \phi^n, \phi^{n-1}\big) \leq \tilde{E}_N\big(\phi^n, \phi^{n-1}, \phi^{n-2}\big) \tag{2.18}$$

for any $\Delta t > 0$, where

$$\begin{aligned}\tilde{E}_N\big(\phi^{n+1}, \phi^n, \phi^{n-1}\big) := E_N\big(\phi^{n+1}\big) &+ \frac{3}{4\Delta t}\big\|\phi^{n+1} - \phi^n\big\|_{-1,N}^2 + \frac{1}{6\Delta t}\big\|\phi^n - \phi^{n-1}\big\|_{-1,N}^2 \\ &+ \frac{1}{2}\Big(\big\|\phi^{n+1} - \phi^n\big\|_2^2 + \big\|\phi^{n+1} - 2\phi^n + \phi^{n-1}\big\|_2^2\Big).\end{aligned} \tag{2.19}$$

Proof. For the energy stability, we take the discrete inner product of (2.14) with $(-\Delta_N)^{-1}(\phi^{n+1} - \phi^n)$

$$\begin{aligned}0 = \frac{1}{\Delta t}\Big\langle \frac{11}{6}\phi^{n+1} - 3\phi^n + \frac{3}{2}\phi^{n-1} - \frac{1}{3}\phi^{n-2}, (-\Delta_N)^{-1}(\phi^{n+1} - \phi^n)\Big\rangle \\ + \big\langle -\Delta_N\big((\phi^{n+1})^3\big), (-\Delta_N)^{-1}(\phi^{n+1} - \phi^n)\big\rangle \\ + \varepsilon^2\big\langle \Delta_N^2\phi^{n+1}, (-\Delta_N)^{-1}(\phi^{n+1} - \phi^n)\big\rangle \\ + A_0\Delta t^2\big\langle \Delta_N^2(\phi^{n+1} - \phi^n), (-\Delta_N)^{-1}(\phi^{n+1} - \phi^n)\big\rangle \\ + \big\langle \Delta_N\big(3\phi^n - 3\phi^{n-1} + \phi^{n-2}\big), (-\Delta_N)^{-1}(\phi^{n+1} - \phi^n)\big\rangle .\end{aligned} \tag{2.20}$$

For the nonlinear term,

$$\begin{aligned}&\big\langle -\Delta_N\big((\phi^{n+1})^3\big), (-\Delta_N)^{-1}(\phi^{n+1} - \phi^n)\big\rangle \\ &= \big\langle (\phi^{n+1})^3, \phi^{n+1} - \phi^n\big\rangle \geq \frac{1}{4}\Big(\|\phi^{n+1}\|_4^4 - \|\phi^n\|_4^4\Big),\end{aligned} \tag{2.21}$$

where the convexity of the function $\frac{1}{4}x^4$ has been applied. For the highest-order linear term,

$$\begin{aligned}&\big\langle \Delta_N^2\phi^{n+1}, (-\Delta_N)^{-1}(\phi^{n+1} - \phi^n)\big\rangle \\ &= \big\langle \nabla_N\phi^{n+1}, \nabla_N(\phi^{n+1} - \phi^n)\big\rangle \\ &= \frac{1}{2}\Big(\big\|\nabla_N\phi^{n+1}\big\|_2^2 - \big\|\nabla_N\phi^n\big\|_2^2 + \big\|\nabla_N(\phi^{n+1} - \phi^n)\big\|_2^2\Big).\end{aligned} \tag{2.22}$$

For the BDF3 temporal stencil, we begin with the following equivalent form:

$$\begin{aligned}&\frac{11}{6}\phi^{n+1} - 3\phi^n + \frac{3}{2}\phi^{n-1} - \frac{1}{3}\phi^{n-2} \\ &= \frac{2}{3}(\phi^{n+1} - \phi^n) + \frac{7}{6}(\phi^{n+1} - 2\phi^n + \phi^{n-1}) + \frac{1}{3}(\phi^{n-1} - \phi^{n-2}).\end{aligned}$$

This in turn indicates that

$$\begin{aligned}
&\left\langle \frac{11}{6}\phi^{n+1} - 3\phi^n + \frac{3}{2}\phi^{n-1} - \frac{1}{3}\phi^{n-2}, (-\Delta_N)^{-1}(\phi^{n+1} - \phi^n) \right\rangle \\
&= \frac{2}{3}\|\phi^{n+1} - \phi^n\|_{-1,N}^2 + \frac{7}{6}\langle \phi^{n+1} - 2\phi^n + \phi^{n-1}, \phi^{n+1} - \phi^n \rangle_{-1,N} \\
&\quad + \frac{1}{3}\langle \phi^{n-1} - \phi^{n-2}, \phi^{n+1} - \phi^n \rangle_{-1,N} \\
&\geq \frac{2}{3}\|\phi^{n+1} - \phi^n\|_{-1,N}^2 - \frac{1}{6}\|\phi^{n+1} - \phi^n\|_{-1,N}^2 - \frac{1}{6}\|\phi^{n-1} - \phi^{n-2}\|_{-1,N}^2 \\
&\quad + \frac{7}{12}\Big(\|\phi^{n+1} - \phi^n\|_{-1,N}^2 - \|\phi^n - \phi^{n-1}\|_{-1,N}^2 + \|\phi^{n+1} - 2\phi^n + \phi^{n-1}\|_{-1,N}^2 \Big) \\
&= \frac{13}{12}\|\phi^{n+1} - \phi^n\|_{-1,N}^2 - \frac{7}{12}\|\phi^n - \phi^{n-1}\|_{-1,N}^2 - \frac{1}{6}\|\phi^{n-1} - \phi^{n-2}\|_{-1,N}^2 \\
&\quad + \frac{7}{12}\|\phi^{n+1} - 2\phi^n + \phi^{n-1}\|_{-1,N}^2. \qquad (2.23)
\end{aligned}$$

For the concave term, the following equivalent expression holds:

$$-3\phi^n + 3\phi^{n-1} - \phi^{n-2} = -\phi^{n+1} + \big(\phi^{n+1} - 2\phi^n + \phi^{n-1}\big) - \big(\phi^n - 2\phi^{n-1} + \phi^{n-2}\big).$$

Then we have

$$\begin{aligned}
&\big\langle \Delta_N(3\phi^n - 3\phi^{n-1} + \phi^{n-2}), (-\Delta_N)^{-1}(\phi^{n+1} - \phi^n) \big\rangle \\
&= \big\langle -3\phi^n + 3\phi^{n-1} - \phi^{n-2}), \phi^{n+1} - \phi^n \big\rangle \\
&= -\big\langle \phi^{n+1} - \phi^n, \phi^{n+1} \big\rangle + \big\langle \phi^{n+1} - \phi^n, \phi^{n+1} - 2\phi^n + \phi^{n-1} \big\rangle \\
&\quad - \big\langle \phi^{n+1} - \phi^n, \phi^n - 2\phi^{n-1} + \phi^{n-2} \big\rangle \\
&\geq -\frac{1}{2}\big(\|\phi^{n+1}\|_2^2 - \|\phi^n\|_2^2\big) - \frac{1}{2}\|\phi^{n+1} - \phi^n\|_2^2 \\
&\quad + \frac{1}{2}\big(\|\phi^{n+1} - \phi^n\|_2^2 - \|\phi^n - \phi^{n-1}\|_2^2\big) - \frac{1}{2}\|\phi^{n+1} - \phi^n\|_2^2 \\
&\quad + \frac{1}{2}\big(\|\phi^{n+1} - 2\phi^n + \phi^{n-1}\|_2^2 - \|\phi^n - 2\phi^{n-1} + \phi^{n-2}\|_2^2\big) \\
&= -\frac{1}{2}\big(\|\phi^{n+1}\|^2 - \|\phi^n\|_2^2\big) - \frac{1}{2}\|\phi^{n+1} - \phi^n\|_2^2 - \frac{1}{2}\|\phi^n - \phi^{n-1}\|_2^2 \\
&\quad + \frac{1}{2}\big(\|\phi^{n+1} - 2\phi^n + \phi^{n-1}\|_2^2 - \|\phi^n - 2\phi^{n-1} + \phi^{n-2}\|_2^2\big). \qquad (2.24)
\end{aligned}$$

Substituting (2.21)-(2.24) into (2.20) yields

$$\begin{aligned}
0 \geq\ & \frac{1}{4}\big(\|\phi^{n+1}\|_4^4 - \|\phi^n\|_4^4\big) + \frac{\varepsilon^2}{2}\big(\|\nabla_N\phi^{n+1}\|_2^2 - \|\nabla_N\phi^n\|_2^2 + \|\nabla_N(\phi^{n+1} - \phi^n)\|_2^2\big) \\
& - \frac{1}{2}\big(\|\phi^{n+1}\|_2^2 - \|\phi^n\|_2^2\big) - \frac{1}{2}\|\phi^{n+1} - \phi^n\|_2^2 \\
& - \frac{1}{2}\|\phi^n - \phi^{n-1}\|_2^2 + A_0\Delta t^2\|\nabla_N(\phi^{n+1} - \phi^n)\|^2
\end{aligned}$$

$$+\frac{1}{\Delta t}\left(\frac{13}{12}\|\phi^{n+1}-\phi^{n}\|_{-1,N}^{2}-\frac{7}{12}\|\phi^{n}-\phi^{n-1}\|_{-1,N}^{2}-\frac{1}{6}\|\phi^{n-1}-\phi^{n-2}\|_{-1,N}^{2}\right)$$
$$+\frac{1}{2}\big(\|\phi^{n+1}-2\phi^{n}+\phi^{n-1}\|_{2}^{2}-\|\phi^{n}-2\phi^{n-1}+\phi^{n-2}\|_{2}^{2}\big). \tag{2.25}$$

This inequality could be rewritten as

$$\begin{aligned}0\geq{}& E_N(\phi^{n+1})-E_N(\phi^{n})+\frac{\varepsilon^2}{2}\|\nabla_N(\phi^{n+1}-\phi^{n})\|_2^2+A_0\Delta t^2\|\nabla_N(\phi^{n+1}-\phi^{n})\|_2^2\\
&+\frac{1}{3\Delta t}\|\phi^{n+1}-\phi^{n}\|_{-1,N}^{2}-\frac{1}{2}\|\phi^{n+1}-\phi^{n}\|_{2}^{2}-\frac{1}{2}\|\phi^{n}-\phi^{n-1}\|_{2}^{2}\\
&+\frac{1}{\Delta t}\left(\frac{3}{4}\|\phi^{n+1}-\phi^{n}\|_{-1,N}^{2}-\frac{7}{12}\|\phi^{n}-\phi^{n-1}\|_{-1,N}^{2}-\frac{1}{6}\|\phi^{n-1}-\phi^{n-2}\|_{-1,N}^{2}\right)\\
&+\frac{1}{2}\big(\|\phi^{n+1}-2\phi^{n}+\phi^{n-1}\|_{2}^{2}-\|\phi^{n}-2\phi^{n-1}+\phi^{n-2}\|_{2}^{2}\big).\end{aligned} \tag{2.26}$$

Under the condition that

$$A_0\geq\frac{9}{32}\varepsilon^{-2}$$

it follows that

$$\frac{\varepsilon^2}{2}+A_0\Delta t^2\geq\sqrt{2A_0}\varepsilon\Delta t\geq\frac{3}{4}\Delta t. \tag{2.27}$$

Therefore, we obtain

$$\begin{aligned}\|\phi^{n+1}-\phi^{n}\|^2&\leq\frac{3}{4}\Delta t\|\nabla_N(\phi^{n+1}-\phi^{n})\|_2^2+\frac{1}{3\Delta t}\|\phi^{n+1}-\phi^{n}\|_{-1,N}^{2}\\
&\leq\frac{\varepsilon^2}{2}\|\nabla_N(\phi^{n+1}-\phi^{n})\|_2^2+A_0\Delta t^2\|\nabla_N(\phi^{n+1}-\phi^{n})\|^2\\
&\quad+\frac{1}{3\Delta t}\|\phi^{n+1}-\phi^{n}\|_{-1,N}^{2},\end{aligned} \tag{2.28}$$

where the Cauchy inequality has been applied. Going back to (2.26), we get

$$\begin{aligned}0\geq{}& E_N(\phi^{n+1})-E_N(\phi^{n})+\frac{1}{2}\big(\|\phi^{n+1}-\phi^{n}\|_{2}^{2}-\|\phi^{n}-\phi^{n-1}\|_{2}^{2}\big)\\
&+\frac{1}{\Delta t}\left(\frac{3}{4}\|\phi^{n+1}-\phi^{n}\|_{-1,N}^{2}-\frac{7}{12}\|\phi^{n}-\phi^{n-1}\|_{-1,N}^{2}-\frac{1}{6}\|\phi^{n-1}-\phi^{n-2}\|_{-1,N}^{2}\right)\\
&+\frac{1}{2}\big(\|\phi^{n+1}-2\phi^{n}+\phi^{n-1}\|_{2}^{2}-\|\phi^{n}-2\phi^{n-1}+\phi^{n-2}\|_{2}^{2}\big),\end{aligned} \tag{2.29}$$

which is equivalent to (2.18). This finishes the proof of Theorem 2.2. □

Corollary 2.1. *Suppose that $A_0\geq\frac{9}{32}\varepsilon^{-2}$ and the initial data are sufficiently regular so that there is a constant $C_0>0$, independent of N and Δt, such that*

$$\begin{aligned}C_0\geq{}& E_N(\phi^{2})+\frac{3}{4\Delta t}\|\phi^{2}-\phi^{1}\|_{-1,N}^{2}+\frac{1}{6\Delta t}\|\phi^{1}-\phi^{0}\|_{-1,N}^{2}\\
&+\frac{1}{2}\big(\|\phi^{2}-\phi^{1}\|_{2}^{2}+\|\phi^{2}-2\phi^{1}+\phi^{0}\|_{2}^{2}\big),\end{aligned} \tag{2.30}$$

where we may assume that initial data, ϕ^0, ϕ^1 and ϕ^2 are mass-conservative Fourier projections of the exact PDE solution, described in Section 3. Then, there is a constant $C_1 > 0$, which depends on Ω and C_0, but is independent of N, Δt and final time, such that

$$\|\phi^m\|_{H_N^1} \le C_1, \quad \forall m \ge 1. \tag{2.31}$$

Proof. By the modified energy inequality (2.18), the following induction analysis could be performed:

$$E_N(\phi^k) \le \tilde{E}_N\big(\phi^k, \phi^{k-1}, \phi^{k-2}\big) \le \cdots \le \tilde{E}_N\big(\phi^2, \phi^1, \phi^0\big) \le C_0, \quad \forall k \ge 2. \tag{2.32}$$

Meanwhile, at each time step t^m, the following inequality comes from an application of quadratic inequality:

$$\frac{1}{4}\|\phi^m\|_4^4 - \|\phi^m\|_2^2 \ge -|\Omega|. \tag{2.33}$$

Then we obtain

$$E_N(\phi^m) \ge \frac{1}{2}\|\phi^m\|_2^2 + \frac{\varepsilon^2}{2}\|\nabla_N \phi^m\|_2^2 - |\Omega|, \tag{2.34}$$

which, in turn, leads to

$$\frac{\varepsilon^2}{2}\big(\|\phi^m\|_2^2 + \|\nabla_N \phi^m\|_2^2\big) \le E_N(\phi^m) + |\Omega| \le C_0 + |\Omega|. \tag{2.35}$$

This is equivalent to

$$\|\phi^m\|_{H_N^1} \le \sqrt{2(C_0 + |\Omega|)\varepsilon^{-2}} =: C_1, \tag{2.36}$$

which is valid for any $m \ge 2$. The case of $m = 1$ is trivial. The proof of Corollary 2.1 is complete. □

Remark 2.2. The requirement (2.27) for the parameter A_0 indicates an order of $A_0 = \mathcal{O}(\varepsilon^{-2})$. Such a requirement is based on a subtle fact that, an extra stability estimate from the surface diffusion term has to be used to balance the stability loss coming from the multi-step explicit treatment of the linear expansive term, and the surface diffusion coefficient is given by ε^2 in the physical parameter. Also see the related work of Douglas-Dupont regularization [44].

On the other hand, such a parameter order $A_0 = \mathcal{O}(\varepsilon^{-2})$ is only used for the theoretical justification of the energy stability. In the practical computations, the choice of $A_0 = \mathcal{O}(1)$ has never led to any energy stability loss for the proposed third order scheme.

Remark 2.3. There have been a few recent works of the second order BDF schemes for certain gradient flow models, such as Cahn-Hilliard [13, 47], epitaxial thin film equation [22, 36, 38], square phase field crystal [16], in which the energy stability was theoretically established. Similarly, a Douglas-Dupont type regularization has to be included in the numerical scheme, while a careful analysis only requires the corresponding parameter A of an order $A = \mathcal{O}(1)$. The primary reason for the difference

in the order of the artificial parameter A between the second and third order numerical schemes is based on the following fact: for the second order scheme, the artificial regularization, with magnitude $\mathcal{O}(\Delta t^2)$, and the temporal discretization terms are sufficient to theoretically justify the energy stability; while for the third order scheme, these two terms are not sufficient to ensure the numerical stability, since the artificial regularization term has to be in the order of $\mathcal{O}(\Delta t^3)$ to keep the third order temporal accuracy.

Remark 2.4. The stability and convergence estimates for the temporally third order accurate numerical schemes have been reported for fluid models, such as viscous Burgers' equation [25], incompressible Navier-Stokes equation [15], harmonic mapping flow [45], etc.

For the gradient models, the only existing works to address the energy stability for a third order numerical scheme could be found [8, 14, 46]. In this article, we provide an alternate third order numerical approach for the standard Cahn-Hilliard equation, for which both the energy stability and optimal rate convergence estimate could be theoretically justified.

Remark 2.5. As a combination of the uniform-in-time H_N^1 bound (2.31) and the discrete Sobolev embedding inequality (2.13), we arrive at a uniform-in-time L_N^6 estimate for the numerical solution

$$\|\phi^m\|_6 \le CC_1, \quad \forall m \ge 1. \tag{2.37}$$

This estimate will be useful in the convergence analysis presented below.

Remark 2.6. In the numerical scheme (2.14), the Douglas-Dupont type regularization term takes the form of $-A_0\Delta t^2\Delta_N(\phi^{n+1}-\phi^n)$, which in turn leads to a parameter order $A_0 = \mathcal{O}(\varepsilon^{-2})$ to ensure the energy stability at a theoretical level. Meanwhile, if higher order regularization term is used, such as the form of $A_0\Delta t^2\Delta_N^2(\phi^{n+1}-\phi^n)$, the artificial parameter could be taken as $A_0 = \mathcal{O}(1)$ to theoretically establish the energy stability analysis; also see the related works [8, 11] for the associated estimates.

2.5. The artificial regularization parameter estimate dependent on the time step size

In a related work [43], a stabilized BDF2 numerical scheme is analyzed for the Cahn-Hilliard equation, and a modified energy stability is theoretically justified under a time step size dependent condition for A_0

$$A_0 \ge \tilde{A}\varepsilon^{-2} - \frac{\alpha_1}{2}\cdot\frac{\varepsilon}{\Delta t} \quad \text{with } \tilde{A} = \mathcal{O}(1), \quad 0 \le \alpha_1 \le 1\,. \tag{2.38}$$

In fact, a similar estimate could also be derived for the proposed BDF3 scheme (2.14).

Theorem 2.3. *Under the condition that*

$$A_0 \geq \frac{9}{8}\varepsilon^{-2} - \frac{3}{4\Delta t}, \tag{2.39}$$

the numerical solution produced by the proposed BDF-type scheme (2.14) *satisfies the modified energy stability estimate* (2.18) *for any* $\Delta t > 0$, *with* $\tilde{E}_N(\phi^{n+1}, \phi^n, \phi^{n-1})$ *defined in* (2.19).

Proof. All the estimate from (2.20) to (2.26) are still valid. For the artificial regularization parameter A_0, we decompose it as $A_0 = A^* - B_0$, with $A^* = \frac{9}{8}\varepsilon^{-2}$, so that $B_0 \leq \frac{3}{4\Delta t}$, $B_0\Delta t \leq \frac{3}{4}$. Then we see that

$$\frac{\varepsilon^2}{2} + A^*\Delta t^2 \geq \sqrt{2A^*}\varepsilon\Delta t \geq \frac{3}{2}\Delta t. \tag{2.40}$$

Moreover, the following lower bound becomes available:

$$\frac{\varepsilon^2}{2} + A_0\Delta t^2 = \frac{\varepsilon^2}{2} + A^*\Delta t^2 - B_0\Delta t^2 \geq \frac{3}{2}\Delta t - \frac{3}{4}\Delta t = \frac{3}{4}\Delta t. \tag{2.41}$$

Because of this bound, the estimates (2.28) and (2.29) are still valid. This finishes the proof of Theorem 2.3. □

With a combination of Theorems 2.2 and 2.3, it is clear that the modified energy stability estimate (2.18) is always valid for

$$A_0 \geq \min\left(\frac{9}{32}\varepsilon^{-2}, \frac{9}{8}\varepsilon^{-2} - \frac{3}{4\Delta t}\right).$$

In turn, we see that the energy stability could be theoretically established even if $A_0 = 0$, under a condition for the time step size, $\Delta t \leq \frac{3}{2}\varepsilon^2$. This fact leads to a more flexible choice of the time step size in the practical computations.

3. The convergence analysis for the third order BDF scheme

The global existence of smooth solution and analytic solution for the CH equation (1.2) has been established in [39]. With initial data of sufficient regularity, we could assume that the exact solution has regularity of class $\mathcal{R}$

$$\phi_e \in \mathcal{R} := H^4(0,T;C^0) \cap H^3(0,T;H^{m+2}) \cap L^\infty(0,T;H^{m+4}). \tag{3.1}$$

Define $\Phi_N(\cdot,t) := \mathcal{P}_N\phi_e(\cdot,t)$, the (spatially-continuous) Fourier projection of the exact solution into $\mathcal{B}^K$, the space of trigonometric polynomials of degree at most K. The following projection approximation is standard: if $\phi_e \in L^\infty(0,T;H^\ell_{\rm per}(\Omega))$, for some $\ell \in \mathbb{N}$, we have

$$\|\Phi_N - \phi_e\|_{L^\infty(0,T;H^k)} \leq Ch^{\ell-k}\|\phi_e\|_{L^\infty(0,T;H^\ell)}, \quad \forall\, 0 \leq k \leq \ell. \tag{3.2}$$

By Φ_N^m we denote $\Phi_N(\cdot\,, t^m)$, with $t^m = m \cdot \Delta t$. Since $\Phi_N \in \mathcal{P}_K$, the mass conservative property is available at the discrete level

$$\overline{\Phi_N^m} = \frac{1}{|\Omega|}\int_\Omega \Phi_N(\cdot, t_m)\, d\mathbf{x} = \frac{1}{|\Omega|}\int_\Omega \Phi_N(\cdot, t_{m-1})\, d\mathbf{x} = \overline{\Phi_N^{m-1}}, \quad \forall m \in \mathbb{N}. \tag{3.3}$$

On the other hand, the initial numerical solutions ϕ^1 and ϕ^2 may be obtained by a stable $RK2$ or $RK3$ algorithm, as described in Remark 2.1, though here, for simplicity, we will assume that they are obtained via mass-conservative Fourier projection of the exact PDE solution. See below. By the mass conservative structure of the gradient flow, we see that $\overline{\phi^2} = \overline{\phi^1} = \overline{\phi^0}$. Therefore, the solution of the numerical scheme (2.14) is also mass conservative at the discrete level

$$\overline{\phi^m} = \overline{\phi^{m-1}}, \quad \forall m \in \mathbb{N}. \tag{3.4}$$

We denote Φ^m as the point projection values of Φ_N at discrete grid points at time instant t^m: $\Phi^m_{i,j,k} := \Phi_N(x_i, y_j, z_k, t^m)$. As indicated before, we use the mass conservative projection for the initial data

$$\phi^\ell_{i,j,k} = \Phi^\ell_{i,j,k} := \Phi_N(x_i, y_j, z_k, t = t_\ell), \quad \ell = 0, 1, 2. \tag{3.5}$$

The error grid function is defined as

$$e^m := \Phi^m - \phi^m, \quad \forall m \geq 0. \tag{3.6}$$

Thus $e^\ell \equiv 0$, $\ell = 0, 1, 2$. A combination of the mass conservative identities, (3.3), (3.4), for the projection solution and numerical solution, respectively, implies that $\overline{e^m} = 0$, for any $m \geq 0$.

For the proposed third order BDF-type scheme (2.14), the convergence result is stated below.

Theorem 3.1. *Given initial data Φ_N^0, Φ_N^1, $\Phi_N^2 \in C_{\text{per}}^{m+4}(\overline{\Omega})$, with periodic boundary conditions, suppose the unique solution for the CH equation* (1.2) *is of regularity class $\mathcal{R}$. Then, provided Δt and h are sufficiently small, for all positive integers ℓ, such that $\Delta t \cdot \ell \leq T$, we have*

$$\|e^\ell\|_2 + \left(\varepsilon^2 \Delta t \sum_{m=1}^{\ell} \|\Delta_N e^m\|_2^2\right)^{\frac{1}{2}} \leq C(\Delta t^3 + h^m), \tag{3.7}$$

where $C > 0$ is independent of Δt and h.

3.1. Review of a preliminary equality

Before the proof of the convergence result, we present the telescope formula in [37] for the third order BDF temporal discretization operator in the following lemma; also see [31,48] for the related discussion. In fact, an inner product with $e^{n+1} + \alpha(e^{n+1} - e^n)$ (with $\alpha > 0$) has also been reported in the analysis for the second order BDF scheme with variable time-step sizes [2, 12], etc.

Lemma 3.1 ([37]). *For the third order BDF temporal discrete operator, there exist constants α_i, $i = 1, \ldots, 10$, $\alpha_1 \neq 0$, such that*

$$\begin{aligned}
&\left\langle \frac{11}{6}e^{n+1} - 3e^n + \frac{3}{2}e^{n-1} - \frac{1}{3}e^{n-2}, 2e^{n+1} - e^n \right\rangle \\
&= \|\alpha_1 e^{n+1}\|_2^2 - \|\alpha_1 e^n\|_2^2 + \|\alpha_2 e^{n+1} + \alpha_3 e^n\|_2^2 - \|\alpha_2 e^n + \alpha_3 e^{n-1}\|_2^2 \\
&\quad + \|\alpha_4 e^{n+1} + \alpha_5 e^n + \alpha_6 e^{n-1}\|_2^2 - \|\alpha_4 e^n + \alpha_5 e^{n-1} + \alpha_6 e^{n-2}\|_2^2 \\
&\quad + \|\alpha_7 e^{n+1} + \alpha_8 e^n + \alpha_9 e^{n-1} + \alpha_{10} e^{n-2}\|_2^2. \qquad (3.8)
\end{aligned}$$

3.2. The proof of convergence theorem

For the Fourier-projected solution Φ_N and its point projection $\Phi_{i,j}^m := \Phi_N(x_i, y_j, t^m)$, a careful consistency analysis implies that

$$\begin{aligned}
&\frac{1}{\Delta t}\left(\frac{11}{6}\Phi^{n+1} - 3\Phi^n + \frac{3}{2}\Phi^{n-1} - \frac{1}{3}\Phi^{n-2}\right) \\
&\quad + \varepsilon^2 \Delta_N^2 \Phi^{n+1} + A_0 \Delta t^2 \Delta_N^2 (\Phi^{n+1} - \Phi^n) \\
&= \Delta_N \cdot \left(\left(\Phi^{n+1}\right)^3 - \left(3\Phi^n - 3\Phi^{n-1} + \Phi^{n-2}\right)\right) + \tau^n \qquad (3.9)
\end{aligned}$$

with $\|\tau^n\|_2 \leq C(\Delta t^3 + h^m)$. In turn, subtracting the numerical scheme (2.14) from the consistency estimate (3.9) yields

$$\begin{aligned}
&\frac{1}{\Delta t}\left(\frac{11}{6}e^{n+1} - 3e^n + \frac{3}{2}e^{n-1} - \frac{1}{3}e^{n-2}\right) \\
&\quad + \varepsilon^2 \Delta_N^2 e^{n+1} + A \Delta t^2 \Delta_N^2 (e^{n+1} - e^n) \\
&= \Delta_N \Big(\left((\Phi^{n+1})^2 + \Phi^{n+1}\phi^{n+1} + (\phi^{n+1})^2\right) e^{n+1} \\
&\qquad - \left(3e^n - 3e^{n-1} + e^{n-2}\right) \Big) + \tau^n. \qquad (3.10)
\end{aligned}$$

Taking a discrete L_N^2 inner product of (3.10) with $2e^{n+1} - e^n$ gives

$$\begin{aligned}
T_0 &:= \frac{1}{\Delta t}\left\langle \frac{11}{6}e^{n+1} - 3e^n + \frac{3}{2}e^{n-1} - \frac{1}{3}e^{n-2}, 2e^{n+1} - e^n \right\rangle \\
&\quad + \varepsilon^2 \big\langle \Delta_N e^{n+1}, \Delta_N (2e^{n+1} - e^n) \big\rangle \\
&\quad + A\Delta t^2 \big\langle \Delta_N (e^{n+1} - e^n), \Delta_N (2e^{n+1} - e^n) \big\rangle \\
&= \Big\langle \left((\Phi^{n+1})^2 + \Phi^{n+1}\phi^{n+1} + (\phi^{n+1})^2\right) e^{n+1} \\
&\qquad - (3e^n - 3e^{n-1} + e^{n-2}), \Delta_N (2e^{n+1} - e^n) \Big\rangle + \big\langle \tau^n, 2e^{n+1} - e^n \big\rangle, \qquad (3.11)
\end{aligned}$$

where summation by parts has been repeatedly applied in the derivation. The local truncation error term could also be bounded in a straightforward way

$$\big\langle \tau^n, 2e^{n+1} - e^n \big\rangle \leq \|\tau^n\|_2^2 + \|e^{n+1}\|_2^2 + \frac{1}{2}\big(\|\tau^n\|_2^2 + \|e^n\|_2^2\big)$$

$$= \frac{3}{2}\|\tau^n\|_2^2 + \|e^{n+1}\|_2^2 + \frac{1}{2}\|e^n\|_2^2. \tag{3.12}$$

The surface diffusion and the Douglas-Dupont regularization terms could be analyzed as follows:

$$\begin{aligned}
&\left\langle \Delta_N e^{n+1}, \Delta_N(2e^{n+1} - e^n)\right\rangle \\
&= \|\Delta_N e^{n+1}\|_2^2 + \left\langle \Delta_N e^{n+1}, \Delta_N(e^{n+1} - e^n)\right\rangle \\
&\geq \|\Delta_N e^{n+1}\|_2^2 + \frac{1}{2}\left(\|\Delta_N e^{n+1}\|_2^2 - \|\Delta_N e^n\|_2^2\right), \qquad (3.13)\\
&\left\langle \Delta_N(e^{n+1} - e^n), \Delta_N(2e^{n+1} - e^n)\right\rangle \\
&= \|\Delta_N(e^{n+1} - e^n)\|_2^2 + \left\langle \Delta_N e^{n+1}, \Delta_N(e^{n+1} - e^n)\right\rangle \\
&\geq \|\Delta_N(e^{n+1} - e^n)\|_2^2 + \frac{1}{2}\left(\|\Delta_N e^{n+1}\|_2^2 - \|\Delta_N e^n\|_2^2\right). \qquad (3.14)
\end{aligned}$$

For the nonlinear error term on the right hand side of (3.11), we recall that

$$\|\Phi^{n+1}\|_6 \leq C_2, \quad \|\phi^{n+1}\|_6 \leq CC_1, \tag{3.15}$$

in which the first inequality comes from the regularity assumption (3.1), while the second one was derived in (2.37) (in Remark 2.5). An application of discrete Hölder inequality leads to

$$\begin{aligned}
&\left\| \left((\Phi^{n+1})^2 + \Phi^{n+1}\phi^{n+1} + (\phi^{n+1})^2\right) e^{n+1}\right\|_2 \\
&\leq \left(\|\Phi^{n+1}\|_6^2 + \|\Phi^{n+1}\|_6 \cdot \|\phi^{n+1}\|_6 + \|\phi^{n+1}\|_6^2\right)\|e^{n+1}\|_6 \\
&\leq \frac{3}{2}\left(\|\Phi^{n+1}\|_6^2 + \|\phi^{n+1}\|_6^2\right)\|e^{n+1}\|_6 \\
&\leq C\left(C_2^2 + C_1^2\right)\|e^{n+1}\|_6. \qquad (3.16)
\end{aligned}$$

Subsequently, we arrive at

$$\begin{aligned}
T_1 &:= \left\langle \left((\Phi^{n+1})^2 + \Phi^{n+1}\phi^{n+1} + (\phi^{n+1})^2\right) e^{n+1} - (3e^n - 3e^{n-1} + e^{n-2}), \Delta_N(2e^{n+1} - e^n)\right\rangle \\
&\leq \left(C\left(C_2^2 + C_1^2\right)\|e^{n+1}\|_6 + 3\|e^n\|_2 + 3\|e^{n-1}\|_2 + \|e^{n-2}\|_2\right) \cdot \left\|\Delta_N(2e^{n+1} - e^n)\right\|_2 \\
&\leq \frac{9}{2}\varepsilon^{-2}\left(C(C_2^2 + C_1^2)\|e^{n+1}\|_6 + 3\|e^n\|_2 + 3\|e^{n-1}\|_2 + \|e^{n-2}\|_2\right)^2 \\
&\quad + \frac{\varepsilon^2}{18}\left\|\Delta_N(2e^{n+1} - e^n)\right\|_2^2 \\
&\leq C\left(C_2^2 + C_1^2\right)\varepsilon^{-2}\|e^{n+1}\|_6^2 + \varepsilon^{-2}\left(36\|e^n\|_2^2 + 36\|e^{n-1}\|_2^2 + 4\|e^{n-2}\|_2^2\right) \\
&\quad + \frac{\varepsilon^2}{18}\left\|\Delta_N(2e^{n+1} - e^n)\right\|_2^2 \\
&\leq C\left(C_2^2 + C_1^2\right)\varepsilon^{-2}\left(\|e^{n+1}\|_2^2 + \|\nabla_N e^{n+1}\|_2^2\right) \\
&\quad + \varepsilon^{-2}\left(36\|e^n\|_2^2 + 36\|e^{n-1}\|_2^2 + 4\|e^{n-2}\|_2^2\right) + \frac{\varepsilon^2}{18}\left\|\Delta_N(2e^{n+1} - e^n)\right\|_2^2
\end{aligned}$$

$$\leq \left(C\left(C_2^4+C_1^4\right)+1\right)\varepsilon^{-6}\|e^{n+1}\|_2^2+\frac{\varepsilon^2}{4}\|\Delta_N e^{n+1}\|_2^2$$
$$+\varepsilon^{-2}\left(36\|e^n\|_2^2+36\|e^{n-1}\|_2^2+4\|e^{n-2}\|_2^2\right)+\frac{\varepsilon^2}{18}\left\|\Delta_N(2e^{n+1}-e^n)\right\|_2^2, \tag{3.17}$$

where the discrete Sobolev inequality (2.13) (in Proposition 2.1) has been applied in the fourth step, and the following estimate has been used in the last step:

$$\|\nabla_N e^{n+1}\|_2^2 \leq \|e^{n+1}\|_2\cdot\|\Delta_N e^{n+1}\|_2$$
$$\leq \frac{\varepsilon^4}{4\alpha}\|\Delta_N e^{n+1}\|_2^2+\alpha\varepsilon^{-4}\|e^{n+1}\|_2^2,\quad \forall\alpha>0. \tag{3.18}$$

Define

$$F^m:=\|\alpha_1 e^m\|_2^2+\|\alpha_2 e^m+\alpha_3 e^{m-1}\|_2^2+\|\alpha_4 e^m+\alpha_5 e^{m-1}+\alpha_6 e^{m-2}\|_2^2, \tag{3.19}$$

in which the parameters α_i correspond to the coefficients in identity (3.8) in Lemma 3.1. Substituting (3.8), (3.12)-(3.14) and (3.17) into (3.11) leads to

$$\begin{aligned}T_2 &:= \frac{1}{\Delta t}(F^{n+1}-F^n)+\frac{3}{4}\varepsilon^2\|\Delta_N e^{n+1}\|_2^2\\ &\quad+\frac{1}{2}(\varepsilon^2+A\Delta t^2)\left(\|\Delta_N e^{n+1}\|_2^2-\|\Delta_N e^n\|_2^2\right)\\ &\leq\left(\left(C\left(C_2^4+C_1^4\right)+1\right)\varepsilon^{-6}+1\right)\|e^{n+1}\|_2^2\\ &\quad+(\varepsilon^{-2}+1)\left(36\|e^n\|_2^2+36\|e^{n-1}\|_2^2+4\|e^{n-2}\|_2^2\right)\\ &\quad+\frac{\varepsilon^2}{18}\left\|\Delta_N(2e^{n+1}-e^n)\right\|_2^2+\frac{3}{2}\|\tau^n\|_2^2.\end{aligned} \tag{3.20}$$

Meanwhile, for the error gradient term $\|\Delta_N(2e^{n+1}-e^n)\|_2^2$, an application of the Cauchy inequality implies that

$$\left\|\Delta_N(2e^{n+1}-e^n)\right\|_2^2\leq 6\|\Delta_N e^{n+1}\|_2^2+3\|\Delta_N e^n\|_2^2. \tag{3.21}$$

Then we arrive at

$$\begin{aligned}T_3 &:= \frac{1}{\Delta t}(F^{n+1}-F^n)+\frac{5}{12}\varepsilon^2\|\Delta_N e^{n+1}\|_2^2\\ &\quad+\frac{1}{2}(\varepsilon^2+A\Delta t^2)\left(\|\Delta_N e^{n+1}\|_2^2-\|\Delta_N e^n\|_2^2\right)\\ &\leq\left(\left(C\left(C_2^4+C_1^4\right)+1\right)\varepsilon^{-6}+1\right)\|e^{n+1}\|_2^2\\ &\quad+(\varepsilon^{-2}+1)\left(36\|e^n\|_2^2+36\|e^{n-1}\|_2^2+4\|e^{n-2}\|_2^2\right)\\ &\quad+\frac{\varepsilon^2}{6}\|\Delta_N e^n\|_2^2+\frac{3}{2}\|\tau^n\|_2^2.\end{aligned} \tag{3.22}$$

Next, let us define

$$\widetilde{F}^m:=F^m+\frac{1}{2}(\varepsilon^2+A\Delta t^2)\Delta t\|\Delta_N e^m\|_2^2. \tag{3.23}$$

Making use of the simple fact

$$\|e^k\|_2^2 \le \frac{1}{\alpha_1^2}\widetilde{F}^k, \quad \forall k \ge 0, \tag{3.24}$$

we obtain the following estimate

$$\begin{aligned} T_4 &:= \frac{1}{\Delta t}(\widetilde{F}^{n+1} - \widetilde{F}^n) + \frac{5}{12}\varepsilon^2\|\Delta_N e^{n+1}\|_2^2 - \frac{\varepsilon^2}{6}\|\Delta_N e^n\|_2^2 \\ &\le \left(\left(C\left(C_2^4 + C_1^4\right) + 1\right)\varepsilon^{-6} + 1\right)\alpha_1^{-2}(\widetilde{F}^{n+1} + \widetilde{F}^n + \widetilde{F}^{n-1} + \widetilde{F}^{n-2}) + \frac{3}{2}\|\tau^n\|_2^2. \end{aligned} \tag{3.25}$$

In turn, an application of discrete Grönwall inequality results in the convergence estimate

$$F^{n+1} + \left(\frac{1}{3}\varepsilon^2\Delta t\sum_{m=1}^{n+1}\|\Delta_N e^m\|_2^2\right)^{\frac{1}{2}} \le \hat{C}(\Delta t^3 + h^m)^2. \tag{3.26}$$

Furthermore, its combination with definition (3.19) (for F^{n+1}) indicates the desired result (3.7). This completes the proof of Theorem 3.1.

4. Numerical results

4.1. Convergence test for the numerical scheme

In this subsection we perform a numerical accuracy check for the third order accurate BDF-type scheme (2.14). The computational domain is set to be $\Omega = (0,1)^2$, and the exact profile for the phase variable is set to be

$$\Phi(x,y,t) = \frac{1}{2\pi}\sin(2\pi x)\cos(2\pi y)\cos(t). \tag{4.1}$$

To make Φ satisfy the original PDE (1.2), we have to add an artificial, time-dependent forcing term. Then the proposed third order BDF-type scheme (2.14) can be implemented to solve for (1.2). To demonstrate the accuracy in time, the spatial numerical error has to be negligible. We fix the spatial resolution as $N = 192$ (so that $h = \frac{1}{192}$), and set the final time $T = 1$. The diffuse interface parameter is taken as $\varepsilon = 0.5$, and we set the artificial regularization parameter as $A_0 = 1$. Naturally, a sequence of time step sizes are taken as $\Delta t = \frac{T}{N_T}$, with $N_T = 100 : 100 : 1000$. The expected temporal numerical accuracy assumption $e = C\Delta t^k$ indicates that $\ln|e| = \ln(CT^k) - k\ln N_T$, so that we plot $\ln|e|$ vs. $\ln N_T$ to demonstrate the temporal convergence order. The fitted line displayed in Fig. 1 shows an approximate slope of -2.9964, which in turn verifies a nice third order temporal convergence order, in both the discrete L_N^2 and L_N^∞ norms.

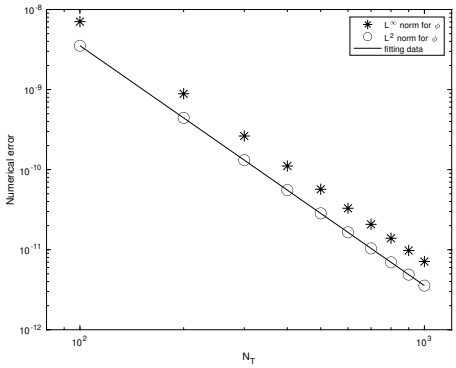

Figure 1: The discrete L_N^2 and L_N^∞ numerical errors vs. temporal resolution N_T for $N_T = 100 : 100 : 1000$, with a spatial resolution $N = 192$. The surface diffusion parameter is taken to be $\varepsilon = 0.5$. The data lie roughly on curves CN_T^{-3}, for appropriate choices of C, confirming the full third-order accuracy of the scheme.

4.2. Numerical simulation of coarsening process and energy dissipation in time

In this subsection we present a numerical simulation result of a physics example. With the assumption that the interface width is in a much smaller scale than the domain size, i.e., $\varepsilon \ll \min\{L_x, L_y\}$, one is interested in how properties associated with the solution to (1.2) scale with time. In particular, the energy dissipation law has attracted a great deal of attentions, and a formal analysis indicates a lower decay bound as $t^{-1/3}$. Meanwhile, it is noted that the rate quoted as the lower bound is typically observed for the averaged values of the energy quantity. A numerical prediction of this scaling law turns out to be very challenging, since a large time scale simulation has to be performed. To adequately capture the full range of coarsening behaviors, numerical simulations for the coarsening process require short- and long-time accuracy and stability, in addition to high spatial accuracy for small values of ε.

We compare the numerical simulation result with the predicted coarsening rate, using the proposed third order scheme (2.14) for the Cahn-Hilliard flow (1.2). The diffusion parameter is taken to be $\varepsilon = 0.02$, and we take the domain as $L_x = L_y = L = 12.8$, $h = \frac{L}{N}$, where h is the uniform spatial step size. For such a value of ε, extensive numerical experiments have shown that $N = 512$ is sufficient to resolve the small structures in the solution.

For the temporal step size Δt, we use increasing values of s in the time evolution. In more detail, $\Delta t = 0.004$ on the time interval $[0, 400]$, $\Delta t = 0.04$ on the time interval $[400, 6000]$, and $\Delta t = 0.16$ on the time interval $[6000, 20000]$. Whenever a new time step size is applied, we initiate the two-step numerical scheme by taking $\phi^{-1} = \phi^{-2} = \phi^0$, with the initial data ϕ^0 given by the final time output of the last time period. Both the energy stability and third order numerical accuracy have been theoretically assured in the previous sections. Fig. 2 presents time snapshots of the phase variable ϕ with $\varepsilon = 0.02$. Significant coarsening is observed in the system. At early times many small

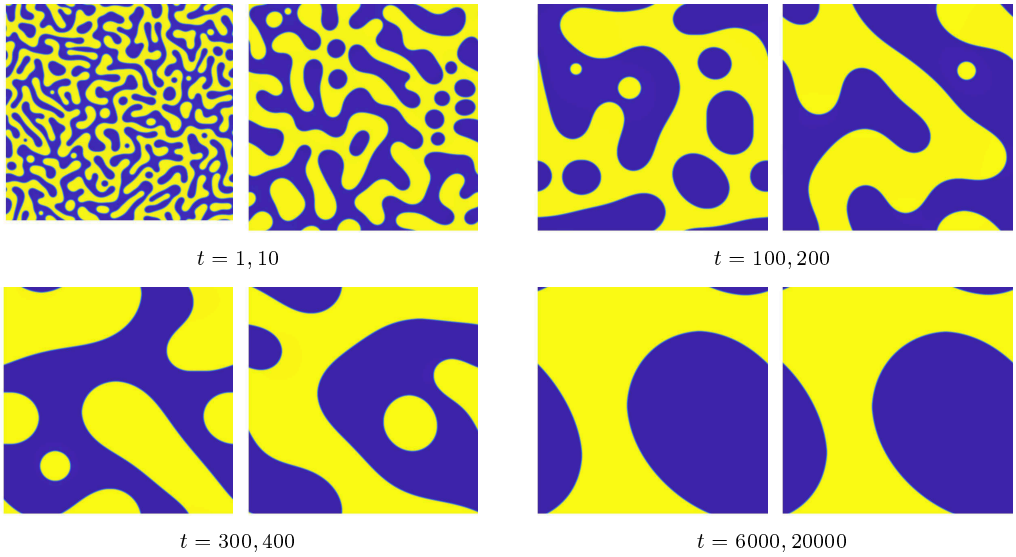

Figure 2: (Color online.) Snapshots of the computed phase variable ϕ at the indicated times for the parameters $L = 12.8$, $\varepsilon = 0.02$.

structures are present. At the final time, $t = 20000$, a single interface structure emerges, and further coarsening is not possible.

The long time characteristics of the solution, especially the energy decay rate, are of interest to material scientists. Recall that, at the space-discrete level, the energy, E_N is defined via (2.12). Fig. 3 presents the log-log plot for the energy versus time, with the given physical parameter $\varepsilon = 0.02$. The detailed scaling "exponent" is obtained using least squares fits of the computed data up to time $t = 160$. A clear observation of the $a_e t^{b_e}$ scaling law can be made, with $a_e = 7.6783$, $b_e = -0.3374$. In other words, an almost perfect $t^{-1/3}$ energy dissipation law is confirmed by our numerical simulation.

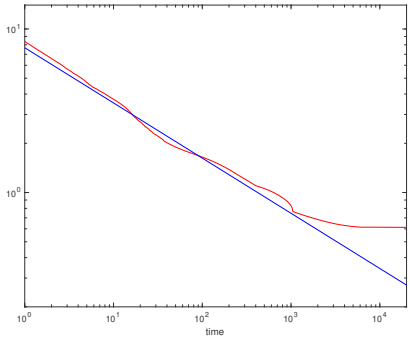

Figure 3: Log-log plot of the temporal evolution the energy E_N for $\varepsilon = 0.02$. The energy decreases like $t^{-1/3}$ until saturation. The red lines represent the energy plot obtained by the simulations, while the straight lines are obtained by least squares approximations to the energy data. The least squares fit is only taken for the linear part of the calculated data, only up to about time $t = 400$. The fitted line has the form $a_e t^{b_e}$, with $a_e = 7.6783$, $b_e = -0.3374$.

Remark 4.1. In this presented numerical simulation, the spatial resolution and time step sizes are taken as the same as the ones presented for a second order accurate, energy stable scheme [17]. For the long time simulation, both numerical schemes have produced similar evolutionary curves in terms of energy. A more detailed calculation shows that long time asymptotic growth rate of the standard deviation given by the third order numerical simulation is closer to $t^{-1/3}$ than that by the second order energy stable scheme: $b_e = -0.3374$, as recorded in Fig. 3, while in [17] this exponent was found to be $b_e = -0.3445$. This gives more evidence that the third order BDF-type scheme is able to produce more accurate long time numerical simulation results than the second order schemes.

5. Concluding remarks

In this article, we propose and analyze a third order accurate BDF-type numerical scheme for the Cahn-Hilliard equation (1.2), combined with Fourier pseudo-spectral spatial discretization. The surface diffusion the nonlinear chemical potential terms are treated implicitly, while the expansive term is approximated by a third order explicit extrapolation formula for the sake of solvability. More importantly, a third order accurate Douglas-Dupont regularization term is added in the numerical scheme. A modified energy stability is theoretically justified, so that a uniform bound for the original energy functional is available, and a theoretical justification of the coefficient A_0 becomes available. Such an energy estimate implies a uniform-in-time L_N^6 bound of the numerical solution. Furthermore, the optimal rate convergence analysis and error estimate are derived in details, with the help of such a uniform L_N^6 bound for the numerical solution. In the convergence estimate, a discrete inner product is taken with an alternate numerical term, to avoid the well-known difficulty associated with the long-stencil nature of the standard BDF3 scheme. Some numerical simulation results are presented to demonstrate the robustness of the numerical scheme and the third order convergence. In particular, the long time simulation results have revealed that, the power index for the energy decay rate for $\varepsilon = 0.02$ (up to $T = 2 \times 10^4$), created by the proposed third order numerical scheme, is more accurate than these created by certain second order accurate, energy stable schemes in the existing literature.

Acknowledgements

This work is supported in part by the Computational Physics Key Laboratory of IAPCAM (P.R. China) under Grant 6142A05200103 (K. Cheng), by the National Science Foundation (USA) under Grant NSF DMS-2012669 (C. Wang), and Grants NSF DMS-1719854, DMS-2012634 (S. Wise).

Appendix A. Proof of Proposition 2.1

Due to the periodic boundary condition for f and its cell-centered representation, it has a corresponding discrete Fourier transformation, as the form given by (2.1)

$$f_{i,j,k} = \sum_{\ell,m,n=-K}^{K} \hat{f}_{\ell,m,n} \exp\big(2\pi \mathrm{i}(\ell x_i + m y_j + n z_k)\big). \tag{A.1}$$

Then we make its extension to a continuous function

$$f_N(x,y,z) = \sum_{\ell,m,n=-K}^{K} \hat{f}_{\ell,m,n} \exp\big(2\pi \mathrm{i}(\ell x + m y + n z)\big). \tag{A.2}$$

The following result is excerpted as [22, Lemma A.2]; similar analyses have also been reported in recent works [17, 21], etc.

Lemma A.1 ([22]). *For $g \in \mathcal{G}_N$, we have*

$$\|g\|_p \le \sqrt{\frac{p}{2}} \|g_N\|_{L^p} \quad \textit{with} \quad p = 4, 6. \tag{A.3}$$

Then we proceed into the proof of Proposition 2.1.

Proof. We see that

$$\begin{aligned} \|f\|_6 &\le \sqrt{3}\|f_N\|_{L^6} \le C\|f_N\|_{H^1} \le C\big(\|f_N\| + \|\nabla f_N\|\big) \\ &= C\big(\|f\|_2 + \|\nabla_N f\|_2\big) \le C\|f\|_{H_N^1}, \end{aligned} \tag{A.4}$$

in which the second step is based on the Sobolev embedding in the continuous space $\|f_N\|_{L^6} \le C\|f_N\|_{H^1}$, and the fourth step comes from the fact that f uniquely corresponds to f_N. This completes the proof of Proposition 2.1. □

References

[1] S. M. Allen and J. W. Cahn, *A microscopic theory for antiphase boundary motion and its application to antiphase domain coarsening*, Acta. Metall. 27 (1979), 1085.

[2] J. Becker, *A second order backward difference method with variable steps for a parabolic problem*, BIT Numer. Math. 38 (1998), 644–662.

[3] J. Boyd, *Chebyshev and Fourier Spectral Methods*, Dover, 2001.

[4] J. Cahn and J. Hilliard, *Free energy of a nonuniform system. I. Interfacial free energy*, J. Chem. Phys. 28 (1958), 258–267.

[5] C. Canuto and A. Quarteroni, *Approximation results for orthogonal polynomials in Sobolev spaces*, Math. Comp. 38 (1982), 67–86.

[6] W. Chen, S. Conde, C. Wang, X. Wang, and S. Wise, *A linear energy stable scheme for a thin film model without slope selection*, J. Sci. Comput. 52 (2012), 546–562.

[7] W. Chen, W. Feng, Y. Liu, C. Wang, and S. Wise, *A second order energy stable scheme for the Cahn-Hilliard-Hele-Shaw equation*, Discrete Contin. Dyn. Syst. Ser. B 24 (2019), 149–182.

[8] W. Chen, W. Li, C. Wang, S. Wang, and X. Wang, *Energy stable higher order linear ETD multi-step methods for gradient flows: application to thin film epitaxy*, Res. Math. Sci. 7 (2020), 13.

[9] W. Chen, C. Wang, S. Wang, X. Wang, and S. Wise, *Energy stable numerical schemes for ternary Cahn-Hilliard system*, J. Sci. Comput. 84 (2020), 27.

[10] W. Chen, C. Wang, X. Wang, and S. Wise, *A linear iteration algorithm for energy stable second order scheme for a thin film model without slope selection*, J. Sci. Comput. 59 (2014), 574–601.

[11] W. Chen, S. Wang, and X. Wang, *Energy stable arbitrary order ETD-MS method for gradient flows with Lipschitz nonlinearity*, CSIAM Trans. Appl. Math. 2 (2021), 460–483.

[12] W. Chen, X. Wang, Y. Yan, and Z. Zhang, *A second order BDF numerical scheme with variable steps for the Cahn-Hilliard equation*, SIAM J. Numer. Anal. 57 (2019), 495–525.

[13] K. Cheng, W. Feng, C. Wang, and S. Wise, *An energy stable fourth order finite difference scheme for the Cahn-Hilliard equation*, J. Comput. Appl. Math. 362 (2019), 574–595.

[14] K. Cheng, Z. Qiao, and C. Wang, *A third order exponential time differencing numerical scheme for no-slope-selection epitaxial thin film model with energy stability*, J. Sci. Comput. 81 (2019), 154–185.

[15] K. Cheng and C. Wang, *Long time stability of high order multi-step numerical schemes for two-dimensional incompressible Navier-Stokes equations*, SIAM J. Numer. Anal. 54 (2016), 3123–3144.

[16] K. Cheng, C. Wang, and S. Wise, *An energy stable Fourier pseudo-spectral numerical scheme for the square phase field crystal equation*, Commun. Comput. Phys. 26 (2019), 1335–1364.

[17] K. Cheng, C. Wang, S. Wise, and X. Yue, *A second-order, weakly energy-stable pseudo-spectral scheme for the Cahn-Hilliard equation and its solution by the homogeneous linear iteration method*, J. Sci. Comput. 69 (2016), 1083–1114.

[18] A. Diegel, X. Feng, and S. Wise, *Convergence analysis of an unconditionally stable method for a Cahn-Hilliard-Stokes system of equations*, SIAM J. Numer. Anal. 53 (2015), 127–152.

[19] A. Diegel, C. Wang, X. Wang, and S. Wise, *Convergence analysis and error estimates for a second order accurate finite element method for the Cahn-Hilliard-Navier-Stokes system*, Numer. Math. 137 (2017), 495–534.

[20] A. Diegel, C. Wang, and S. Wise, *Stability and convergence of a second order mixed finite element method for the Cahn-Hilliard equation*, IMA J. Numer. Anal. 36 (2016), 1867–1897.

[21] W. Feng, A. Salgado, C. Wang, and S. Wise, *Preconditioned steepest descent methods for some nonlinear elliptic equations involving p-Laplacian terms*, J. Comput. Phys. 334 (2017), 45–67.

[22] W. Feng, C. Wang, S. Wise, and Z. Zhang, *A second-order energy stable Backward Differentiation Formula method for the epitaxial thin film equation with slope selection*, Numer. Methods Partial Differential Equations 34 (2018), 1975–2007.

[23] D. Gottlieb and S. Orszag, *Numerical Analysis of Spectral Methods, Theory and Applications*, SIAM, 1977.

[24] S. Gottlieb, F. Tone, C. Wang, X. Wang, and D. Wirosoetisno, *Long time stability of a classical efficient scheme for two dimensional Navier-Stokes equations*, SIAM J. Numer.

Anal. 50 (2012), 126–150.
[25] S. Gottlieb and C. Wang, *Stability and convergence analysis of fully discrete Fourier collocation spectral method for 3-D viscous Burgers' equation*, J. Sci. Comput. 53 (2012), 102–128.
[26] Z. Guan, J. Lowengrub, and C. Wang, *Convergence analysis for second order accurate schemes for the periodic nonlocal Allen-Cahn and Cahn-Hilliard equations*, Math. Methods Appl. Sci. 40 (2017), 6836–6863.
[27] Z. Guan, J. Lowengrub, C. Wang, and S. Wise, *Second-order convex splitting schemes for nonlocal Cahn-Hilliard and Allen-Cahn equations*, J. Comput. Phys. 277 (2014), 48–71.
[28] J. Guo, C. Wang, S. Wise, and X. Yue, *An H^2 convergence of a second-order convex-splitting, finite difference scheme for the three-dimensional Cahn-Hilliard equation*, Commun. Math. Sci. 14 (2016), 489–515.
[29] J. Guo, C. Wang, S. Wise, and X. Yue, *An improved error analysis for a second-order numerical scheme for the Cahn-Hilliard equation*, J. Comput. Appl. Math. 388 (2021), 113300.
[30] D. Han and X. Wang, *A second order in time, uniquely solvable, unconditionally stable numerical scheme for Cahn-Hilliard-Navier-Stokes equation*, J. Comput. Phys. 290 (2015), 139–156.
[31] Y. Hao, Q. Huang, and C. Wang, *A third order BDF energy stable linear scheme for the no-slope-selection thin film model*, Commun. Comput. Phys. 29 (2021), 905–929.
[32] J. Hesthaven, S. Gottlieb, and D. Gottlieb, *Spectral Methods for Time-dependent Problems*, Cambridge University Press, 2007.
[33] D. Li and Z. Qiao, *On second order semi-implicit Fourier spectral methods for 2D Cahn-Hilliard equations*, J. Sci. Comput. 70 (2017), 301–341.
[34] D. Li and Z. Qiao, *On the stabilization size of semi-implicit Fourier-spectral methods for 3D Cahn-Hilliard equations*, Commun. Math. Sci. 15 (2017), 1489–1506.
[35] D. Li, Z. Qiao, and T. Tang, *Characterizing the stabilization size for semi-implicit Fourier-spectral method to phase field equations*, SIAM J. Numer. Anal. 54 (2016), 1653–1681.
[36] W. Li, W. Chen, C. Wang, Y. Yan, and R. He, *A second order energy stable linear scheme for a thin film model without slope selection*, J. Sci. Comput. 76 (2018), 1905–1937.
[37] J. Liu, *Simple and efficient ale methods with provable temporal accuracy up to fifth order for the stokes equations on time varying domains*, SIAM J. Numer. Anal. 51 (2013), 743–772.
[38] X. Meng, Z. Qiao, C. Wang, and Z. Zhang, *Artificial regularization parameter analysis for the no-slope-selection epitaxial thin film model*, CSIAM Trans. Appl. Math. 1 (2020), 441–462.
[39] K. Promislow, *Time analyticity and Gevrey regularity for solutions of a class of dissipative partial differential equations*, Nonlinear Anal. 16 (1991), 959–980.
[40] J. Shen and J. Xu, *Convergence and error analysis for the scalar auxiliary variable (SAV) schemes to gradient flows*, SIAM J. Numer. Anal. 56 (2018), 2895–2912.
[41] J. Shen, J. Xu, and J. Yang, *The scalar auxiliary variable (SAV) approach for gradient flows*, J. Comput. Phys. 353 (2018), 407–416.
[42] J. Shen, J. Xu, and J. Yang, *A new class of efficient and robust energy stable schemes for gradient flows*, SIAM Review 61 (2019), 474–506.
[43] L. Wang and H. Yu, *On efficient second order stabilized semi-implicit schemes for the Cahn-Hilliard phase-field equation*, J. Sci. Comput. 77 (2018), 1185–1209.
[44] X. Wu, G. van Zwieten, and K. van der Zee, *Stabilized second-order convex splitting schemes for Cahn-Hilliard models with application to diffuse-interface tumor-growth models*, Int. J. Numer. Methods Biomed. Eng. 30 (2014), 180–203.

[45] Z. Xia, C. Wang, L. Xu, and Z. Zhang, *A third order accurate in time, fourth order finite difference scheme for the harmonic mapping flow*, J. Comput. Appl. Math. 401 (2022), 113766.
[46] C. Xu and T. Tang, *Stability analysis of large time-stepping methods for epitaxial growth models*, SIAM J. Numer. Anal. 44 (2006), 1759–1779.
[47] Y. Yan, W. Chen, C. Wang, and S. Wise, *A second-order energy stable BDF numerical scheme for the Cahn-Hilliard equation*, Commun. Comput. Phys. 23 (2018), 572–602.
[48] C. Yao, C. Wang, Y. Kou, and Y. Lin, *A third order linearized BDF scheme for Maxwell's equations with nonlinear conductivity using finite element method*, Int. J. Numer. Anal. Model. 14 (2017), 511–531.